Chemico-Biological Interactions 179 (2009) 321–328

Contents lists available at ScienceDirect

Chemico-Biological Interactions

journal homepage: www.elsevier.com/locate/chembioint

Structure–function roles of four cysteine residues in the human arsenic (+3 oxidation state) methyltransferase (hAS3MT) by site-directed mutagenesis

Xiaoli Song[a], Zhirong Geng[a], Jingshu Zhu[a], Chengying Li[a], Xin Hu[b], Ningsheng Bian[a], Xinrong Zhang[c], Zhilin Wang[a,*]

[a] State Key Laboratory of Coordination Chemistry, School of Chemistry and Chemical Engineering, Nanjing University, Hankou Road 22, Nanjing 210093, PR China
[b] Modern Analysis Center of Nanjing University, Nanjing 210093, PR China
[c] Key Laboratory for Atomic and Molecular Nanosciences of Education Ministry, Department of Chemistry, Tsinghua University, Beijing 100084, PR China

ARTICLE INFO

Article history:
Received 12 October 2008
Received in revised form 13 December 2008
Accepted 29 December 2008
Available online 10 January 2009

Keywords:
Structure–function roles
Activity cites
Cysteine residues
Human arsenic methyltransferase
Arsenic
Site-directed mutagenesis

ABSTRACT

Cysteine (Cys) residues are often crucial to the function and structure of proteins. Cys157 and Cys207 in recombinant mouse arsenic (+3 oxidation state) methyltransferase (AS3MT) are shown to be related to enzyme activity and considered to be the catalytic sites. The roles of some conserved Cys residues in the N-terminal region of the rat AS3MT also have been examined. However, little is known about the roles of the Cys residues in the middle region. The metabolism of inorganic arsenic in human is different from rat and mouse in some aspects though the AS3MT has a high degree of similarity in these species. In order to determine whether the Cys156 and Cys206 (corresponding to the catalytic sites, Cys157 and Cys207 in the mouse AS3MT) in the hAS3MT act as the catalytic sites and to study the roles of the Cys residues (Cys226 and Cys250) near the catalytic center in the middle region, we designed and prepared four mutants (C156S, C206S, C226S, and C250S) in which one Cys residue replaced by serine by PCR-based site-directed mutagenesis. The native form and cysteine/serine mutants were assayed for enzyme activity, free thiols, and the secondary structures by circular dichroism and Fourier transform infrared. Our data show that, besides C156S and C206S, C250S is another potential important site. C226S seems to have the same action as the wild-type hAS3MT with the consistent K_M and V_{max} values. Meanwhile, selenium can also inhibit the methylation of inorganic arsenic by C226S. All the mutants except C226S are calculated to have dramatic changes in the secondary structures. Cys250 might form an intramolecular disulfide bond with another Cys residue. These findings demonstrate that Cys residues at positions 156, 206, and 250 play important roles in the enzymatic function and structure of the hAS3MT.

1. Introduction

Inorganic arsenic (iAs) is a potent human carcinogen. More recent epidemiological studies have demonstrated that there is an increased risk for cancers of urinary bladder, lungs, skin, and possibly also kidneys and liver in people chronic exposed to iAs in occupational and environmental settings [1]. Generally, iAs is converted into monomethylated arsenicals (MMA) and dimethylated arsenicals (DMA) by the catalysis of arsenic (3+) methyltransferase (AS3MT) in humans and many other species. However, the formation of trimethylated arsenicals (TMA) is extensive in rat. TMA are also detected in the urine of patients in a rare subacute arsenic poisoning accident [2]. However, this is not prevalent. The pathway for the transformation of iAs into these metabolites can be summarized as $iAs^{5+} \rightarrow iAs^{3+} \rightarrow MMA^{5+} \rightarrow MMA^{3+} \rightarrow DMA^{5+} \rightarrow DMA^{3+}$, in which iAs^{3+} is the substrate, the final products are trivalent and the process is described as an oxidative methylation mechanism [3,4]. Another putative enzymatic mechanism is put forward as $iAs^{5+} \rightarrow iAs^{3+} \rightarrow ATG^{3+}$ (arsenic triglutathione) $\rightarrow MADG^{3+}$ (monomethylarsonic diglutathione) $\rightarrow MMA^{3+} \rightarrow MMA^{5+}$ and $iAs^{5+} \rightarrow iAs^{3+} \rightarrow ATG^{3+} \rightarrow MADG^{3+} \rightarrow DAMG^{3+}$ (dimethylarsinic glutathione) $\rightarrow DMA^{3+} \rightarrow DMA^{5+}$, in which arsenic-GSH complexes are directly methylated by the hAS3MT to produce MMA^{3+} and DMA^{3+}, $MADG^{3+}$ is the substrate for further methylation rather than MMA^{3+} and pentavalent compounds are the final metabolites

Abbreviations: iAs, inorganic arsenic; MMA, monomethylated arsenicals; DMA, dimethylated arsenicals; TMA, trimethylated arsenicals; AS3MT, arsenic (3+) methyltransferase; IPTG, isopropyl β-D-thiogalactopyranoside; BSA, bovine serum albumin; SAM, , S-adenosylmethionine; Cys, cysteine; ATG, arsenic triglutathione; MADG, monomethylarsonic diglutathione; DAMG, dimethylarsinic glutathione; DTNB, 5,5′-dithiobis (2-nitrobenzoic acid); CD, circular dichroism; ATR-FTIR, attenuated total reflection Fourier transform infrared; WT, wild-type; GSH, glutathione; PBS, phosphate buffer solution; HPLC–ICP-MS, high performance liquid chromatography–inductively coupled plasma-mass spectrometry; SDS-PAGE, sodium dodecyl sulfate-polyacrylamide gel electrophoresis.

* Corresponding author. Tel.: +86 25 83686082; fax: +86 25 83317761.
E-mail address: wangzl@nju.edu.cn (Z. Wang).

0009-2797/$ – see front matter © 2009 Elsevier Ireland Ltd. All rights reserved.
doi:10.1016/j.cbi.2008.12.018

[5]. Commonly, methylated arsenicals are thought to be less toxic and methylation of iAs has been considered to be a detoxification reaction [6]. Whereas, metabolites containing As^{3+} are more cytotoxic, genotoxic and more potent enzyme inhibitors than iAs [7–11]. It has been suggested that there is large inter-individual variation in arsenic metabolism [12,13], which may be related to the genetic polymorphisms of the enzymes participating in iAs methylation. In these processes, AS3MT catalyzes S-adenosylmethionine (SAM)-dependent methylation and the transformation of As^{5+} to As^{3+}. Some researchers described that, similarly to other arsenate reductases, AS3MT used thioredoxin or glutaredoxin to translate As^{5+} to As^{3+} in vivo [14]. However, the mechanisms governing the methylation of iAs by AS3MT remain unclear.

Different from other amino acids, cysteine (Cys) residues are often conserved and act importantly in the structure and function of proteins. Cys residues which are critical to protein function are usually used at enzyme catalytic sites. A Cys pair may form a disulfide bond for stabilizing protein structure [15–17] and many additional roles of Cys residues have been described. Lately, Cys157 and Cys207 in recombinant mouse AS3MT have been revealed to be related to enzyme activity. In the protein model, the topology supports the formation of an intramolecular disulfide bond by these two active-site Cys residues during the catalytic cycle [15]. The roles of some conserved Cys residues (32, 61, 85, and 156) in the N-terminal region of the rat AS3MT have been examined and C156S is completely inactive. In the C-terminal portion common to rat, mouse, and human, there are seven additional conserved Cys residues, including a CysCys pair. This region is required for protein stabilization and enzyme activity [16]. As homologous protein, there is only one aspartic acid missing in the hAS3MT, but the activity is different in some aspects. Otherwise, the effects of the catalytic sites on the structure of the AS3MT have not been reported at the present time. These findings led us to investigate whether the Cys156 and Cys206 in the hAS3MT also act as the catalytic sites and whether they affect the structure of the hAS3MT as well as to study the roles of the Cys residues (Cys226 and Cys250) near the catalytic center in the middle region.

In the work reported here, we have used recombinant DNA techniques to study the roles of four Cys residues (Cys156, Cys206, Cys226, and Cys250) in the hAS3MT by substituting serine for each Cys residue and then measuring the mutants (C156S, C206S, C226S, and C250S) functions including enzyme activity, and varieties in the secondary structures by circular dichroism (CD) and attenuated total reflection Fourier transform infrared (ATR-FTIR). In addition, since DTNB has been extensively used for probing free thiol groups in proteins, we also used this reagent to measure the concentration of free thiol groups in the wild-type (WT) hAS3MT and the mutants. Of these, except C226S, all other mutants displayed dramatic changes in the secondary structures and enzyme activity. The results of this study documented the roles of each of the four Cys residues in the hAS3MT.

2. Materials and methods

Caution: iAs has been classified as a human carcinogen and should be handled accordingly.

2.1. Materials

Restriction enzymes, dNTPs and PrimeSTAR HS DNA Polymerase were from Takara. The wild-type (WT) hAS3MT expression plasmid, pET-32a-hAS3MT, was available from an earlier study. Expression host, *E. coli* BL21 (DE3) pLysS was got from Novagen. Isopropyl β-D-thiogalactopyranoside (IPTG), 5,5′-dithiobis (2-nitrobenzoic acid) (DTNB), bovine serum albumin (BSA), SAM, and selenium were bought from Sigma. All other reagents were of analytical grade and all solutions were prepared using Milli-Q deionized water. The phosphate buffer solutions (PBS) were prepared from Na_2HPO_4 and NaH_2PO_4.

Table 1
Primers used for site-directed mutagenesis.

	Primer	Sequence
C156S	+	5′GGCACAAGGTTAATAAC**GCT**GTTTGATAC3′
	–	5′GTATCAAAC**AGC**GTTATTAACCTTGTGCC3′
C206S	+	5′ATAAAGCACCACCCAG**GCT**CTCACCCC3′
	–	5′GGGGTGAG**AGC**CTGGGTGGTGCTTTAT3′
C226S	+	5′GACCAAACGTGGAGG**GCT**GAACCCA3′
	–	5′CCTTGCTCAAAAAATTGGGTTC**AGC**CCTCC3′
C250S	+	5′GAAACAAAACG**GCT**GTCACCGATAAC3′
	–	5′TGGAAAGAGTTATCGGTGAC**AGC**CG3′

Bold and underlined letters indicate the mutation sites introduced by PCR-based mutagenesis. (+) Sense strand; (–) antisense strand.

2.2. Preparation of hAS3MT mutants

The cDNA encoding for the WT hAS3MT carried in the plasmid pET-32a-hAS3MT [18] was used to generate the hAS3MT mutants. *E. coli* BL21 (DE3) pLysS was used for protein production. Substitutions of serine for Cys156, Cys206, Cys226, and Cys250 of the hAS3MT were carried using site-directed mutagenesis by PCR overlap extension with pET-32a-hAS3MT as the DNA template. The primers used for the mutagenesis are listed in Table 1 with the mutated codons underlined. The oligonucleotide primers, each complementary to opposite strands of the hAS3MT gene sequence, were extended during temperature cycling (30 cycles of PCR consisting of incubation for 10 s at 98 °C, 15 s at 55 °C, and 1 min at 72 °C) and final extension (7 min at 72 °C) for one cycle by using PrimeSTAR HS DNA Polymerase. Incorporation of the oligonucleotide primers generated the mutants with Cys to serine substitution for the hAS3MT. Following mutagenesis the target PCR products were purified by agarose gel DNA purification kit and sequenced using the double-stranded dideoxy method to ensure that no errors had been introduced during the amplification process [19]. For expression the recombinant plasmids were transformed into *E. coli* BL21 (DE3) pLysS.

2.3. Expression and purification of hAS3MT mutants

The colonies were selected on standard ampicillin-containing agar plates. Single colonies were picked, and in each case the fidelity of the PCR amplification and the presence of the mutation were confirmed by sequencing [19]. The expression and purification of the hAS3MT mutants (C156S, C206S, C226S, and C250S) followed protocols used for the WT hAS3MT [18]. Briefly, the transformed cells were grown in 200 ml LB broth medium (10 g tryptone, 5 g yeast extract, 10 g NaCl per 1 l) containing 100 μg/ml of ampicillin at 25 °C until OD_{600} reached 0.8–1.0 and protein expression was induced by the addition of 1 mM IPTG for an additional 4 h at 25 °C. The cultured cells were harvested by centrifugation at 7000 rpm for 10 min at 4 °C and then resuspended in 20 ml 1× binding buffer (20 mM Tris–HCl buffer at pH 7.9 containing 0.5 M NaCl and 5 mM imidazole). After sonication on ice and centrifugation at 12,000 rpm for 15 min at 4 °C, the cleared lysate was filtered through a 0.45 μm membrane and loaded onto a 2.5 ml Ni-NTA agarose column which had been equilibrated with 1× binding buffer to purify the target protein. The enzyme was eluted with 1× elute buffer (20 mM Tris–HCl buffer at pH 7.9 containing 0.5 M NaCl and 1 M imidazole). The purity of each enzyme was confirmed by SDS-PAGE. Compared with the other mutants, it was necessary to use a lower concentration IPTG (0.5 mM) and was induced

overnight at 20 °C when C250S was expressed. The enzymes were dialyzed twice against PBS to remove imidazole. Protein concentration was determined by the Bradford assay based on a BSA standard curve.

2.4. Steady-state enzyme activity assays and kinetic measurements

Enzyme activity of the WT hAS3MT and the mutants was determined by using HPLC–ICP-MS. Enzyme reactions were carried out in 100 μl of 25 mM PBS (pH 7.0), 11 μg enzyme, 7 mM GSH, and varying amounts of iAs^{3+} substrate and SAM. To measure iAs^{3+} substrate kinetics, 1 mM SAM and 0.5–600 μM iAs^{3+} were used. In SAM kinetic experiments, 1 μM iAs^{3+} and 0.05–0.3 mM SAM were used. The reaction mixtures were incubated at 37 °C for the desired time and then quenched by boiling the samples for 5 min. The samples were analyzed before (to determine the concentrations of the pentavalent arsenicals) and after (to determine the total arsenicals) being treated with H_2O_2 at a final concentration of 3% to convert all arsenic metabolites to pentavalency [5]. The H_2O_2-treated samples were then boiled again for 5 min. The concentrations of trivalent arsenicals were calculated by the differences between the total and the pentavalent arsenicals. After centrifugation at 12,000 rpm for 10 min and being filtered through a 0.22 μm pore membrane, 20 μl aliquots of reaction mixtures were separated on an anion-exchange column (PRP X-100 250 mm × 4.6 mm i.d., 5 μm, Hamilton) using 15 mM $(NH_4)_2HPO_4$, adjusted to pH 6.0 with H_3PO_4, as the mobile phase with the flow rate of 1.2 ml/min. Arsenicals of the separated species were detected by an Elan9000 ICP-MS. The amounts of arsenic species were calculated with the working curves prepared using 10, 20, 40, 80, and 160 ppb of standard arsenic species. Methylation rates were calculated as mole equivalents of methyl groups transferred from SAM to iAs^{3+} (i.e., 1 pmol CH_3 per 1 pmol MMA or 2 pmol CH_3 per 1 pmol DMA) [20].

2.5. Antagonism effects of selenium on iAs^{3+} methylation by C226S

The antagonism effects of selenium on iAs^{3+} methylation catalyzed by C226S were determined through the reactions (100 μl) containing 25 mM PBS (pH 7.0), 11 μg C226S, 7 mM GSH, 1 mM SAM, and varying amounts of iAs^{3+} and 0, 1, 2 μM selenium. The samples were treated with H_2O_2 at a final concentration of 3% to convert all arsenic metabolites to pentavalency and then analyzed by HPLC–ICP-MS (conditions were consistent with 2.4). Methylation rates were calculated as mole equivalents of methyl groups transferred from SAM to iAs^{3+} as above.

2.6. Circular dichroism measurements and secondary structure analysis

CD (195–250 nm) spectra were recorded on a JASCO-J810 Spectropolarimeter (Jasco Co., Japan) in a cell of 1 mm slit width and 10 mm light length. The scanning rate was set at 50 nm/min. The spectra were the average of three readings. Standard measurements were carried out at room temperature in very dilute enzyme solutions (2 μM) (25 mM PBS at pH 7.0). A blank spectrum of PBS was collected previously and the subtraction was automatically carried out to get the protein spectrum. No baseline drifts were observed during the collection time of a complete spectrum. The secondary structure parameters of the WT hAS3MT and the mutants were estimated with the Jasco secondary structure manager software using the reference CD data—Yang. jwr [21].

2.7. ATR-FTIR spectroscopy and secondary structure analysis

All spectra were obtained at room temperature with an infrared spectrometer (Bruker, IFS 66/s) equipped with a deuterated triglyceride sulfate (DTGS) detector and coupled with an ATR device. All measurements were performed in PBS 25 mM at pH 7.0. The concentration of the WT hAS3MT and the mutants for FTIR spectroscopic measurements was 2.0×10^{-4} M. A 256-scan water vapor correction spectrum was collected previously and the correction was automatically carried out during data collection. After an open background spectrum was recorded, the sample solution was spread on the ZnSe wafer and its 256-scan spectrum was collected at a resolution of 4 cm^{-1}. The protein spectrum was obtained by subtracting the spectrum of PBS. Baseline correction was carried out in the range from 1700 to 1600 cm^{-1} to get amide I bands. Fourier self-deconvolution and secondary derivative were applied to the range to estimate the position and strength of the component bands. According to these parameters, curve-fitting process was carried out by origin software (version 7.0) to get the best Gaussian-shaped curves that fit the original protein spectrum. Assignment and integration of each absorption band gave the relative contents of different types of secondary structures.

2.8. Titration of free thiol groups with DTNB

The concentration of free thiol groups of the WT hAS3MT and the mutants was determined by the method of Ellman [22]. The reaction mixture, which was placed in a cuvet, contained 4×10^{-4} μmol of enzymes in 1.0 ml of 0.05 M Tris–HCl buffer, pH 8.0, and 10 μl of 0.01 M DTNB in 0.05 M PBS, pH 7.0. The reaction was carried out at 25 °C, and the release of 2-nitro-5-mercaptobenzoic acid was followed at 412 nm, using LAMBDA-35 spectrometer. The concentration of free thiol groups was calculated with the working curves prepared using 0.5, 1, 2.5, 5, 10, and 20 μM of Cys.

3. Results and discussion

3.1. Recombinant hAS3MT cysteine/serine mutants

Methylation of iAs is the main biotransformation in animals and fungi. An enzyme encoded by *Cyt19* gene catalyzes the methylation of iAs to MMA, DMA, and TMA [23]. However, the methyltransferase activity is lacking in some mammals such as chimpanzee [24], marmoset, tamarin monkey [25], and guinea pig [26,27]. These differences are possibly due to the genetic modification of the enzyme. Cys residues often play important roles in the structure and function of enzymes. Dmitri E. Fomenko shows that Cys157 and Cys207 in recombinant mouse AS3MT are the catalytic sites. Substitution of Cys156 with serine in recombinant rat AS3MT also makes it inactive. To further determine whether the corresponding Cys residues (Cys156 and Cys206) in the hAS3MT are related to its activity and to study the effects of the Cys residues (Cys226 and Cys250) near the activity sites in the middle region on the enzyme activity, we prepared four hAS3MT mutants (C156S, C206S, C226S, and C250S) by PCR-based site-directed mutagenesis. A variety of bacteria growth temperatures and times were compared. Growth and induction at 25 °C produced enough soluble protein when the C156S, C206S, and C226S mutants were expressed. However, the C250S mutant had to be expressed in a modified way at a lower temperature (20 °C) as compared to the other enzyme variants. This probably attributes to that the substitution of Cys250 by serine absolutely destroys the structure of the hAS3MT and makes it easier to form inclusion body than the other mutants during expression. A lower temperature is required to slow down

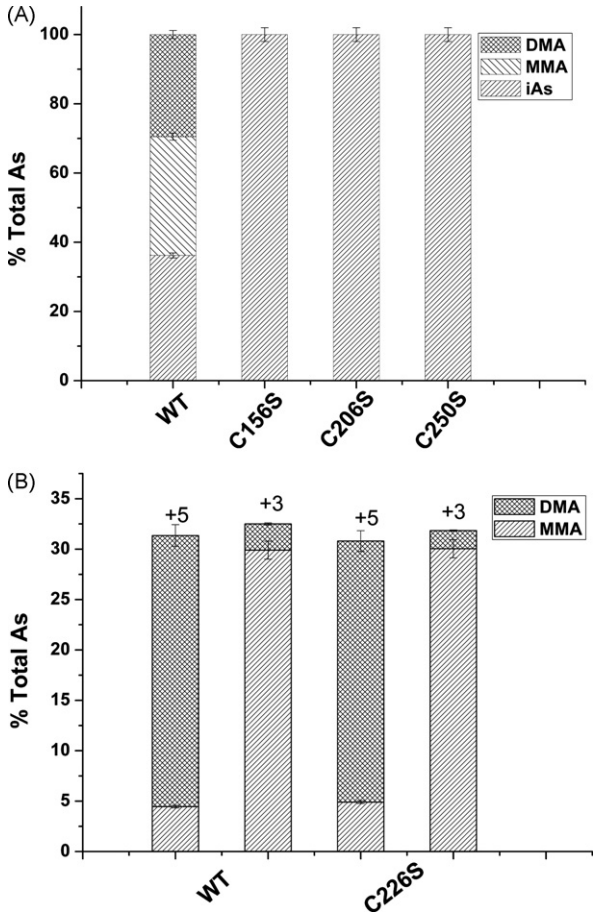

Fig. 1. (A) Effects of C156S, C206S, and C250S mutation on the catalytic activity of the hAS3MT. Reaction mixtures containing 11 μg enzymes, 1 μM iAs^{3+}, 1 mM SAM, 7 mM GSH, 25 mM PBS (pH 7.0) with the WT hAS3MT or mutants (C156S, C206S, and C250S) were cultured at 37 °C for 2 h with H_2O_2 treating. (B) Effects of C226S mutation on the catalytic activity of the hAS3MT. Reaction mixtures containing 11 μg enzymes, 1 μM iAs^{3+}, 1 mM SAM, 7 mM GSH, 25 mM PBS (pH 7.0) with C226S or the WT hAS3MT were cultured at 37 °C for 2 h with or without H_2O_2 treating before analyzed by HPLC–ICP-MS. Data are presented as the means ± S.E. of four separate experiments.

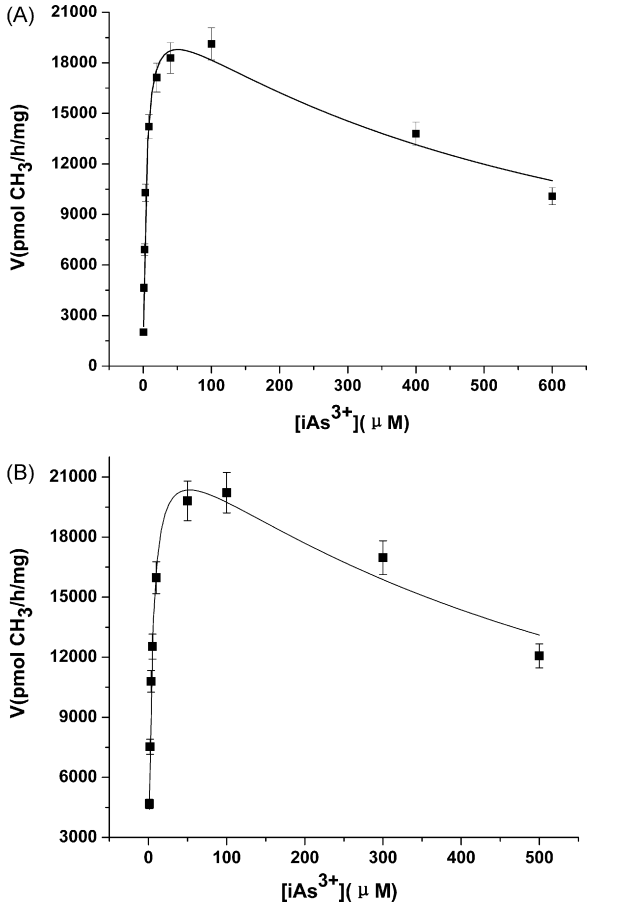

Fig. 2. Concentration dependence of rate. (A) WT hAS3MT and (B) C226S reaction mixtures containing 11 μg enzymes, 1 mM SAM, 7 mM GSH, and 25 mM PBS (pH 7.0) were incubated with the concentrations of iAs^{3+} indicated for 2 h with H_2O_2 treating. Values are the means ± S.D. of three separate experiments. The lines show the least squares fit of Eq. (1) to the data.

the formation speed of this mutant to gain soluble protein. All the mutant proteins were successfully overexpressed. The purity of each mutant protein was confirmed to be over 95% by SDS-PAGE (data not shown).

3.2. Kinetic properties of the WT hAS3MT and the mutants

Through the same reaction mixtures (100 μl of 25 mM PBS (pH 7.0), 11 μg enzyme, 7 mM GSH, 1 μM iAs^{3+}, 1 mM SAM) incubated at 37 °C for 2 h, we compared the activity and catalytic capacity of the hAS3MT native form and the mutants. Unexpectedly, except C156S and C206S, C250S was also completely inactive in iAs^{3+} methylation, while the WT hAS3MT could convert about 65% iAs^{3+} into methylated arsenicals with approximately 35% MMA^{5+} and 30% DMA^{5+} (Fig. 1A) within 2 h. This result suggests that Cys250 is similarly critical for enzyme function. In contrast, C226S performed the same as the WT hAS3MT, verifying that Cys226 is probably not concerned with catalysis directly (Fig. 1B). DMA mainly existed in pentavalent form while MMA in trivalent form in both the reactions catalyzed by the WT hAS3MT or C226S. The iAs^{3+} concentration range investigated here with the WT hAS3MT or C226S clearly shows both substrate inhibition of rate by iAs^{3+} (Fig. 2A and B). The rate of methylation in the presence of noncompetitive substrate inhibition [28] is defined in Eq. (1):

$$V = \frac{[S]V_{max}}{K_M + [S] + ([S]^2/K_I)} \quad (1)$$

where V is the initial velocity of the reaction (pmolCH_3transferred/(h mg protein)), $[S]$ the substrate (iAs^{3+}) concentration (μM), V_{max} the maximal velocity of the reaction (pmolCH3transferred/(h mg protein)), K_M the Michaelis constant for iAs^{3+} (μM), and K_I is the inhibition constant for iAs^{3+} (μM) [29]. The kinetic parameters estimated by fitting the Eq. (1) are listed in Table 2. Double reciprocal plots of the relation between the concentrations of iAs^{3+} and the rate (Fig. 3A and B) also give us the same results (Table 2). The K_M of SAM calculated from the double reciprocal plots of the dependence of the reaction rate on the concentrations of SAM (Fig. 4) is 47.84 μM for the WT hAS3MT and 51.01 μM for C226S. The K_M values of iAs^{3+} and SAM for the WT hAS3MT and C226S agree well with each other. The maximal velocity is also consistent. That no significant differences are observed between the kinetic parameters suggests the same activity of the WT hAS3MT and C226S (Table 2). Cys157 and Cys207 are the catalytic sites of the mouse AS3MT and are speculated to form an intramolecular disulfide bond during the catalytic cycle [15]. Based on our kinetic data presented here and corresponded to the study of the mouse AS3MT, we can conclude that Cys156 and Cys206 are the active sites of the hAS3MT. When one of these two Cys residues is substituted by serine, the intramolecular disulfide bond cannot be formed and the methylation will no longer carry

Table 2
Kinetic parameters for iAs^{3+} methylation by WT hAS3MT and C226S.

	hAS3MT		C226S	
	Eq. (1)	Drp	Eq. (1)	Drp
V_{max} (pmol/(h mg))	21,170 ± 1,079	19,836 ± 919	23,500 ± 1,124	21,556 ± 1,092
K_M (μM)	3.20 ± 0.24	3.19 ± 0.17	3.71 ± 0.23	3.60 ± 0.19
K_I (mM)	0.70 ± 0.09		0.66 ± 0.13	

Values represent the mean ± S.D. of three independent determinations. Eq. (1) represents the kinetic parameters of iAs^{3+} estimated from the data in Fig. 2 by Eq. (1) using orign8.0. Drp represents the parameters of iAs^{3+} calculated from the data in Fig. 3.

out. Interestingly, Cys250 is another potential important residue of the hAS3MT since substitution of it by serine also makes the enzyme inactive. However, Cys226 does not affect the function of the hAS3MT.

3.3. Effects of Cys226 on the antagonism of selenium against iAs^{3+} methylation

Selenium and arsenic act as metabolic antagonists [30]. Selenium has been shown to modulate the activity of AS3MT [31]. To assess whether the replacement of Cys226 affects the antagonism of Se^{4+} against iAs^{3+} methylation, we conducted an investigation of the kinetic properties of C226S in the presence of Se^{4+}. A double-reciprocal plot shows that Se^{4+} is an inhibitor of iAs^{3+} methylation catalyzed by C226S as well (Fig. 5). The K_i (inhibition constant for Se^{4+}) value calculated from the replot of the slopes of the corresponding double reciprocal plots vs. the concentrations of Se^{4+} (Fig. 5 inset) is 2.50 μM for C226S and is consistent with that for the WT hAS3MT (2.61 μM) [18]. Some researchers speculated that Se^{4+} might bind to Cys residues of the AS3MT during the inhibition reaction. The consistent K_i value of Se^{4+} for the WT hAS3MT and C226S indicates that Cys226 is not the binding site for Se^{4+} inhibition of iAs^{3+} methylation. There must be some other Cys residues for the binding.

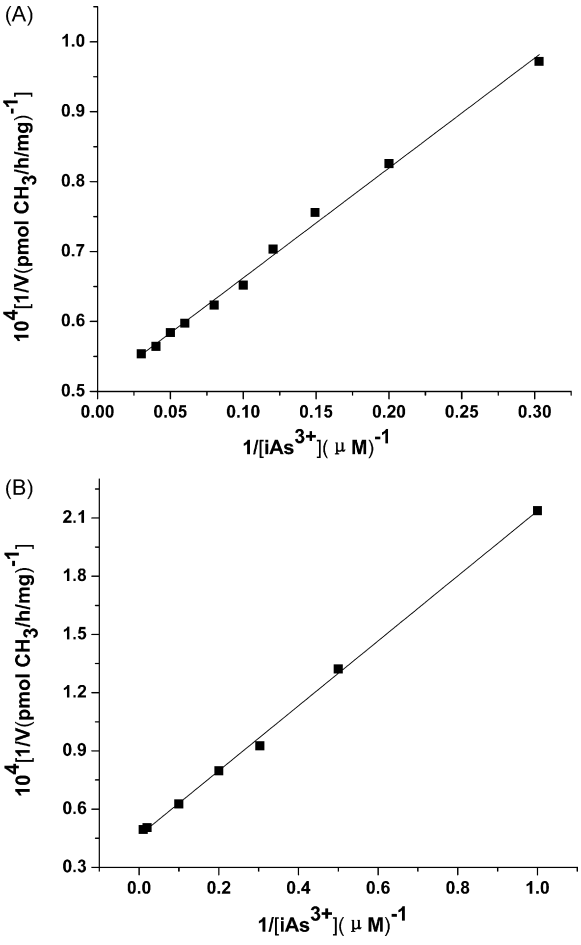

Fig. 3. Double reciprocal plots of the relation between the concentration of iAs^{3+} and the rate. (A) WT hAS3MT and (B) C226S reaction mixtures containing 11 μg enzymes, 1 mM SAM, 7 mM GSH, and 25 mM PBS (pH 7.0) with iAs^{3+} indicated were incubated at 37 °C for 2 h with H_2O_2 treating.

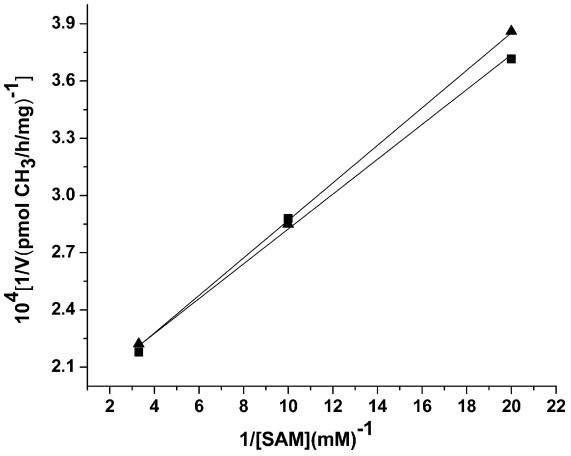

Fig. 4. Double reciprocal plots of the relation between the concentration of SAM and the rate. (■) WT hAS3MT; (▲) C226S reaction mixtures containing 11 μg enzymes, 1 μM iAs^{3+}, 7 mM GSH, 25 mM PBS (pH 7.0) with SAM indicated were incubated at 37 °C for 2 h with H_2O_2 treating.

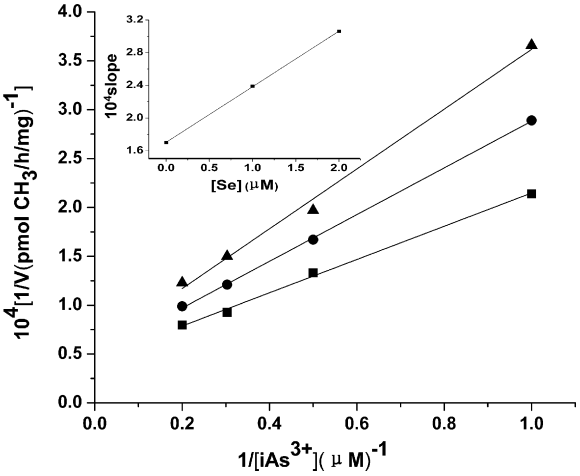

Fig. 5. Double reciprocal plots for the inhibition of iAs^{3+} methylation by Se^{4+} with C226S. The reaction mixtures containing 11 μg C226S, 1 mM SAM, 7 mM GSH, 25 mM PBS (pH 7.0) with iAs^{3+} indicated were incubated at 37 °C for 1.5 h with H_2O_2 treating. Plots for 0 μM (■), 1 μM (●), and 2 μM (▲) Se^{4+}. Replot of slopes vs. concentration of inhibitor is shown in the inset.

Table 3
Secondary structures of WT hAS3MT and the mutants estimated from CD spectroscopy.

	α (%)	β (%)	Turn (%)	Random (%)
WT	29.0 ± 2.2	23.9 ± 1.9	17.9 ± 1.7	29.2 ± 1.4
C156S	30.1 ± 2.9	14.0 ± 1.6	23.2 ± 2.1	32.6 ± 3.4
C206S	36.7 ± 3.1	17.8 ± 1.8	18.6 ± 2.3	26.9 ± 3.6
C250S	43.7 ± 2.6	2.30 ± 0.2	28.8 ± 3.1	25.2 ± 1.1
C226S	29.5 ± 2.7	22.8 ± 1.9	19.0 ± 1.3	29.7 ± 2.5

Values represent the mean ± S.D. of three independent experiments. The parameters were analyzed with the Jasco secondary structure manager with the reference CD data—Yang. jwr in 25 mM (pH 7.0), PBS at room temperature.

3.4. Secondary structures of the enzymes determined by circular dichroism

Compared with other amino acids, Cys residues are often significant to proteins, especially to some redox-active proteins. They may act as the catalytic sites or a Cys pair may stabilize protein structure by forming a disulfide bond. The translation from As^{3+} to As^{5+}

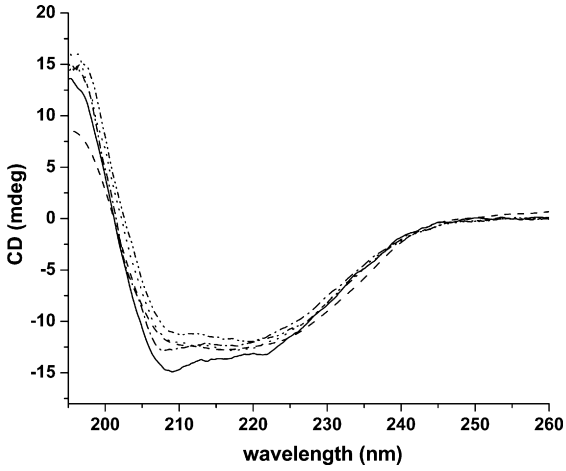

Fig. 6. CD spectra of the WT hAS3MT and the mutants. Spectra were taken at protein concentration of 2 μM. WT, solid line; C156S, dashed line; C206S, dotted line; C226S, dashed-dotted line; C250S, dashed-dotted-dotted line.

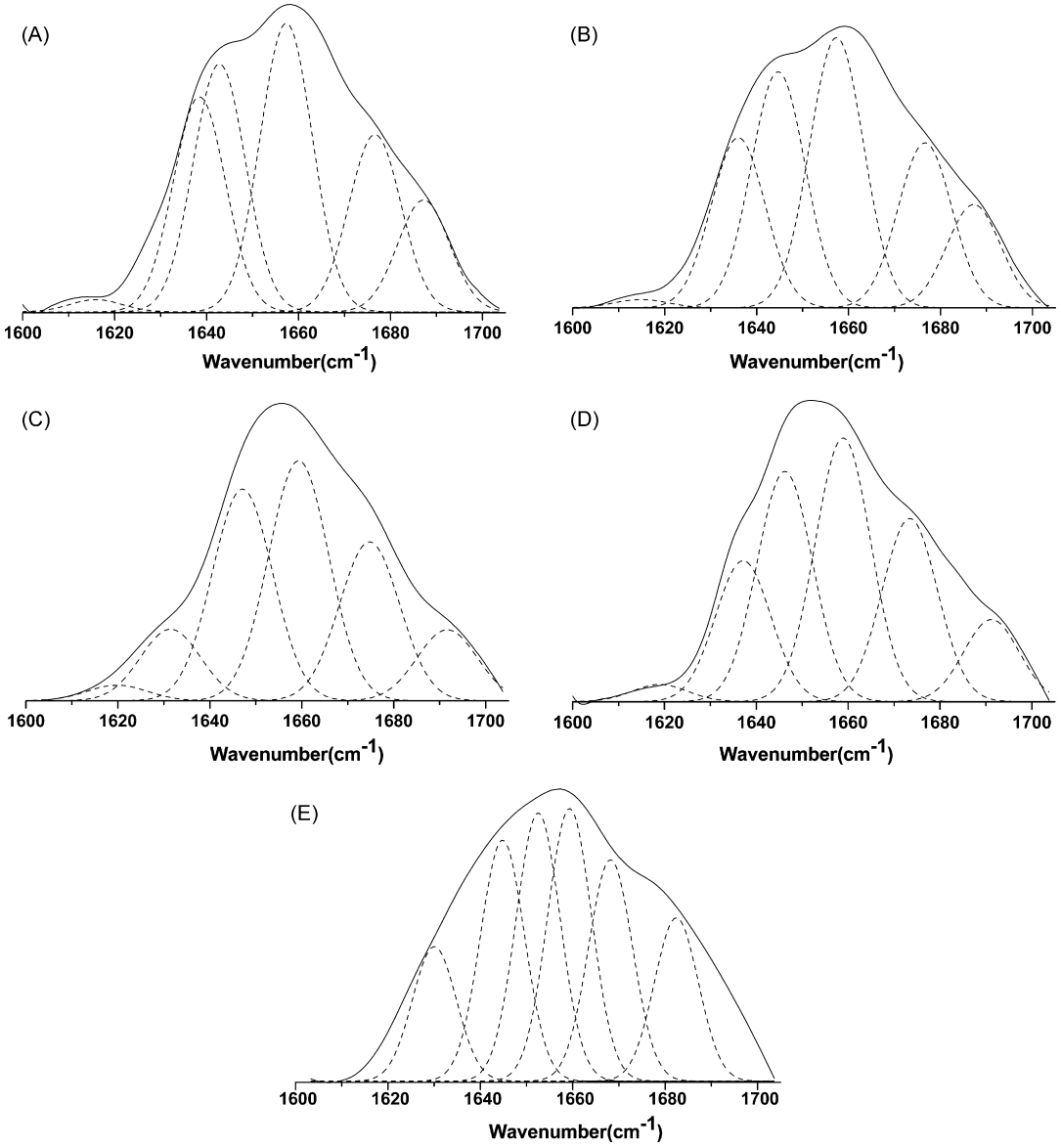

Fig. 7. The curve-fitted amide I region of the WT hAS3MT (A), C226S (B), C156S (C), C206S (D), and C250S (E). The component peaks are the result of curve fitting using a Gaussian shape. The continuous lines represent the experimental FTIR spectra after Savitzky–Golay smoothing; the dashed lines represent the fitted components.

is probably owing to the redox-active Cys residues in the hAS3MT. The deactivation of Cys mutants may result from conformational changes because of the rupture of disulfide bond. CD is more sensitive to protein secondary structure [32–34]. We used CD spectrum to monitor the secondary structure and analyzed the contents of four secondary structures with the Jasco secondary structure manager software using the reference CD data—Yang. jwr in 25 mM PBS (pH 7.0) at room temperature (Table 3). The spectra of the WT hAS3MT and the mutants are shown in Fig. 6. The spectra of the WT hAS3MT and C226S are indicative of α + β structures [35]. The WT hAS3MT was analyzed to have the secondary structures of 29.0% α-helix, 23.9% β-pleated sheet, 17.9% β-turn, and 29.2% random coil. The content of α-helix increased in C156S while the β-pleated sheet decreased remarkably by 41.4%; in C206S, both α-helix and β-pleated sheet changed obviously by 26.5% increased and 25.52% decreased respectively; surprisingly, there was only 2.3% β-pleated sheet preserving in C250S while α-helix had increased to 43.7%; however, the contents of the secondary structures in C226S had little change in all the forms. According to the structural model of the mouse AS3MT [15], we speculate that the Cys156 and Cys206 are in the β-pleated sheet domain and locate in a well-defined cavity structure in the hAS3MT. The substitution of these two Cys residues (Cys156 and Cys206) by serine may change the circumstance of this β-pleated sheet domain and makes the content of β-pleated sheet decrease very obviously. From our data, we can see that the secondary structures of C250S change much more than the other mutants. Based on our above report (a lower temperature is needed to express C250S and it is also inactive in iAs^{3+} methylation) and the CD data, we can surmise that Cys250 might form an intramolecular disulfide bond which acts importantly in the structure maintenance of the hAS3MT. The rupture of this intramolecular disulfide bond, resulted from the substitution of Cys250 by serine, leads to the dramatic changes of the secondary structures of the hAS3MT and makes the C250S mutant inactive. However, Cys226 may just keep alone from other Cys residues.

3.5. Secondary structures of the enzymes determined by ATR-FTIR

FTIR spectroscopy has been shown to be a powerful technique in some cases to determine the structure of proteins. The so-called amide I bands in the IR spectrum is primarily the C=O stretching vibrations of the amide groups, and located approximately between 1700 and 1600 cm^{-1}. It is believed that such amide I bands are sensitive to the secondary structures of proteins, enzymes, and polypeptides [36–38]. The original and curve-fitting spectra of the WT hAS3MT and the mutants are exhibited in Fig. 7. For the quantitative analysis of each secondary structure, Fourier self-deconvolution and second derivative were applied to amide I bands to estimate the number and position of component bands [39,40]. Six component bands were determined in amide I and curve-fitting process was iterated to achieve the best fitted curves. The component bands were attributed according to the well-established assignment criterion [41]. The bands ranging 1610–1640 cm^{-1} were generally assigned to β-pleated sheet, 1640–1650 cm^{-1} to random coil, 1650–1658 cm^{-1} to α-helix, and 1660–1700 cm^{-1} to β-turn structure. According to the assignments, the percentages of each secondary structure of the enzymes calculated from the integrated areas of the component bands in amide I are listed in Table 4. The WT hAS3MT in PBS buffer solution contained α-helix 26.6% (1657 cm^{-1}), β-sheet 21.4% (1600–1640 cm^{-1}), β-turn 23.5% (1660–1700 cm^{-1}), and random 28.5% (1643 cm^{-1}). The C226S mutant revealed a very similar spectrum with the WT hAS3MT. In the Cys156 and Cys206 mutants, the content of β-pleated sheet decreased, while that of α-helix increased in trend. The number and the position of the components of these two mutants in amide I region were similar to those of the WT hAS3MT. Thus, assignments for bands observed in the derivatives were carried out in the same way. However, the result of the C250S mutant was significantly different as compared to the WT hAS3MT. There was only one band observed around 1629 cm^{-1} with 7% β-pleated sheet left. While the content of α-helix increased to 45.8% calculated from two bands at 1653 cm^{-1} and 1659 cm^{-1}. Here, though the second band was at 1659 cm^{-1}, we assigned it to the α-helix since the content of α-helix is 43.7% from our CD data and in some cases, the peak around 1659 cm^{-1} was empirically assigned to the α-helix [42]. It should be noted that the contents of the four secondary structures of the WT hAS3MT and the mutants estimated from FTIR spectroscopy are in good agreement with those estimated from CD spectroscopy.

Table 4
Secondary structures of WT hAS3MT and the mutants estimated from FTIR spectroscopy.

	α (%)	β (%)	Turn (%)	Random (%)
AMT	26.6 ± 3.6	20.7 ± 4.6	24.2 ± 3.2	28.5 ± 4.9
C156S	33.0 ± 4.0	10.3 ± 2.7	24.5 ± 3.6	32.2 ± 1.6
C206S	33.9 ± 5.3	17.2 ± 2.5	23.8 ± 4.2	25.1 ± 2.9
C250S	45.8 ± 5.7	6.0 ± 3.8	27.5 ± 3.2	20.7 ± 4.4
C226S	28.2 ± 3.2	20.4 ± 2.7	24.0 ± 2.3	27.4 ± 4.1

Values represent the mean ± S.D. of three independent experiments.

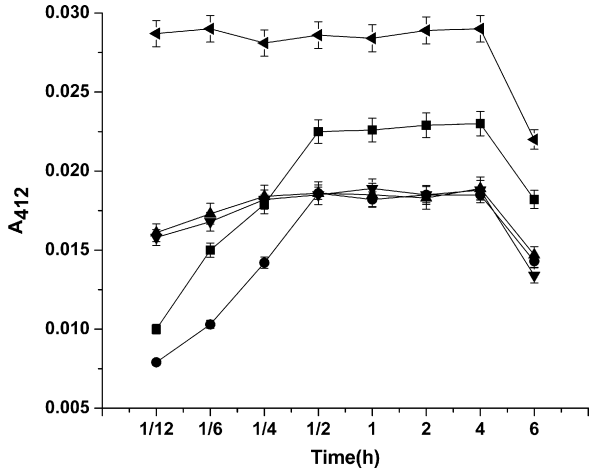

Fig. 8. Absorbance vs. time for the enzymes treated with DTNB. Plots for WT (■), C226S (●), C156S (▲), C206S (▼), and C250S (◄).

3.6. Concentration of free thiol groups in the WT hAS3MT and the mutants

Titration of solutions of the WT hAS3MT or the mutants showed that the rate of reaction of the free thiol groups with DTNB, as measured by the release of 2-nitro-5-thiobenzoic acid followed at 412 nm, was different in the same solutions containing equivalent 4×10^{-4} μmol enzymes (Fig. 8). The thiol contents of the

Table 5
Thiol group concentration of the WT hAS3MT and the mutants.

Enzyme	Thiol group/Mol of Enzyme
WT	4.42 ± 0.32[a]
C226S	3.33 ± 0.27[a]
C156S	3.47 ± 0.30[b]
C206S	3.39 ± 0.32[b]
C250S	5.22 ± 0.41[b]

Values represent the mean ± S.E. of six independent experiments.
[a] Determined by the reaction incubated at 25 °C for 30 min.
[b] Determined by the reaction incubated at 25 °C for 15 min.

enzymes are listed in Table 5. The rate of reaction of the free thiol groups with DTNB was similar in the WT AS3MT and C226S but markedly increased in the other mutants. This result indicates that the secondary structure of the C156S, C206S, and C250S mutants is different from that of the WT hAS3MT and agrees well with our previous findings obtained from the CD and FTIR spectroscopy. The content of thiols was more in C250S while less in the other mutants than that in the equivalent WT hAS3MT. Since free thiol is only contained in free Cys residues in proteins, we speculate that Cys250 forms an intramolecular disulfide bond with another Cys in the WT hAS3MT and the substitution of it with serine makes the other Cys residue free. Cys156, Cys206, and Cys226 do not form intramolecular disulfide bond with other Cys residues. These results are also consistent with our CD and FTIR data.

4. Conclusions

In summary, this study of the Cys residues in the hAS3MT has indicated that Cys156 and Cys206 act as the enzyme activity sites; Cys250 might be essential for the maintenance of the enzyme stability by forming an intramolecular disulfide bond with another potential Cys residues; Cys226 does not join in a disulfide bond and is not the binding site for Se^{4+} in the inhibition of iAs^{3+} methylation. All the mutants except C226S are calculated to have dramatic changes in the secondary structures as compared with the WT hAS3MT. This report here also demonstrates the relationship between structure and activity of the hAS3MT. Since no high-resolution crystal structure of the hAS3MT has been described, these data provide an alternative approach to understand how Cys residues contribute to the structure and function of this important arsenic methylation enzyme.

Conflict of interest

None declared.

Acknowledgments

We greatly appreciate the National Natural Science Foundation of China (20535020, 20671051, 90813020, and 20721002) and National Basic Research Program of China (2007CB925102).

References

[1] National Research Council, Essentiality and Therapeutic Uses, Arsenic in Drinking Water, National Academy Press, Washington, DC, 1999, pp. 251–263.
[2] Y.Y. Xu, Y. Wang, Q.M. Zheng, B. Li, X. Li, Y.P. Jin, X.Q. Lv, G. Qu, G.F. Sun, Clinical manifestations and arsenic methylation after a rare subacute arsenic poisoning accident, Toxicol. Sci. 103 (2008) 278–284.
[3] W.R. Cullen, B.C. McBride, J. Reglinski, The reduction of trimethylarsine oxide to trimethylarsine by thiols: a mechanistic model for the biological reduction of arsenicals, J. Inorg. Biochem. 21 (1984) 45–60.
[4] H.V. Aposhian, Enzymatic methylation of arsenic species and other new approaches to arsenic toxicity, Annu. Rev. Pharmacol. Toxicol. 37 (1997) 397–419.
[5] T. Hayakawa, Y. Kobayashi, X. Cui, S. Hirano, A new metabolic pathway of arsenite: arsenic–glutathione complexes are substrates for human arsenic methyltransferase Cyt19, Arch. Toxicol. 79 (2005) 183–191.
[6] T.W. Gebel, Arsenic methylation is a process of detoxification through accelerated excretion, Int. J. Hyg. Environ. Health 205 (2002) 505–508.
[7] S. Nesnow, B.C. Roop, G. Lambert, M. Kadiiska, R.P. Mason, W.R. Cullen, M.J. Mass, DNA damage induced by methylated trivalent arsenicals is mediated by reactive oxygen species, Chem. Res. Toxicol. 12 (2002) 1627–1634.
[8] M. Styblo, L.M. DelRazo, L. Vega, D.R. Germolec, E.L. LeCluyse, G.A. Hamilton, W. Reed, C.Q. Wang, W.R. Cullen, D.J. Thomas, Comparative toxicity of trivalent and pentavalent inorganic and methylated arsenicals in rat and human cells, Arch. Toxicol. 74 (2000) 289–299.
[9] D.J. Thomas, M. Styblo, S. Lin, The cellular metabolism and systemic toxicity of arsenic, Toxicol. Appl. Pharmacol. 176 (2001) 127–144.
[10] M.J. Mass, A. Tennant, B.C. Roop, W.R. Cullen, M. Styblo, D.J. Thomas, A.D. Kligerman, Methylated trivalent arsenic species are genotoxic, Chem. Res. Toxicol. 14 (2001) 355–361.
[11] T. Schwerdtle, I. Walter, I. Mackiw, A. Hartwig, Induction of oxidative DNA damage by arsenite and its trivalent and pentavalent methylated metabolites in cultured human cells and isolated DNA, Carcinogenesis 24 (2003) 967–974.
[12] M. Vahter, Genetic polymorphism in the biotransformation of inorganic arsenic and its role in toxicity, Toxicol. Lett. 112–113 (2000) 209–217.
[13] J.S. Chung, D.A. Kalman, L.E. Moore, M.J. Kosnett, A.P. Arroyo, M. Beeris, D.N. Mazumder, A.L. Hernandez, A.H. Smith, Family correlations of arsenic methylation patterns in children and parents exposed to high concentrations of arsenic in drinking water, Environ. Health Perspect. 110 (2002) 729–733.
[14] R. Mukhopadhyay, B.P. Rosen, Arsenate reductases in prokaryotes and eukaryotes, Environ. Health Perspect. 110 (Suppl. 5) (2002) 745–748.
[15] D.E. Fomenko, W.B. Xing, B.M. Adair, D.J. Thomas, V.N. Gladyshev, High-throughput identification of catalytic redox-active cysteine residues, Science 315 (2007) 387–389.
[16] J.X. Li, S.B. Waters, Z. Drobna, V. Devesa, M. Styblob, D.J. Thomas, Arsenic (+3 oxidation state) methyltransferase and the inorganic arsenic methylation phenotype, Toxicol. Appl. Pharmacol. 204 (2005) 164–169.
[17] M. Beeby, B.D. O'Connor, C. Ryttersgaard, D.R. Boutz, L.J. Perry, The Genomics of disulfide bonding and protein stabilization in thermophiles, PLoS Biol. 3 (2005) 1549–1558.
[18] Z.R. Geng, X.L. Song, Z. Xing, J.L. Geng, S.C. Zhang, X.R. Zhang, Z.L. Wang, Effects of selenium on the structure and function of recombinant human S-adenosyl-L-methionine dependent arsenic (III) methyltransferase in *E. coli*, J. Biol. Inorg. Chem., doi:10.1007/s00775-008-0464-6.
[19] F. Sanger, S. Nicklen, A.R. Coulson, DNA sequencing with chain-terminating inhibitors, Proc. Natl. Acad. Sci. U.S.A. 7 (1977) 5463–5467.
[20] F.S. Walton, S.B. Waters, S.L. Jolley, E.L. LeCluyse, D.J. Thomas, M. Styblo, Selenium compounds modulate the activity of recombinant rat As^{III}-methyltransferase and the methylation of arsenite by rat and human hepatocytes, Chem. Res. Toxicol. 16 (2003) 261–265.
[21] Y.T. Yang, C.S.C. Wu, H.M. Martinez, Calculation of protein conformation from circular dichroism, Methods Enzymol. 130 (1986) 208–257.
[22] G.L. Ellman, Tissue sulfhydryl groups, Arch. Biochem. Biophys. 82 (1959) 70–77.
[23] S. Lin, Q. Shi, F.B. Nix, M. Styblo, M.A. Beck, K.M. Herbin-Davis, L.L. Hall, J.B. Simeonsson, D.J. Thomas, A novel S-adenosyl-L-methionine: arsenic(III) methyltransferase from rat liver cytosol, J. Biol. Chem. 277 (2002) 10795–10803.
[24] M. Vahter, Species differences in the metabolism of arsenic compounds, Appl. Organomet. Chem. 8 (1994) 175–182.
[25] R.A. Zakharyan, E. Wildfang, H.V. Aposhian, Enzymatic methylation of arsenic compounds. III. The marmoset and tamarin, but not the rhesus monkey, are deficient in methyltransferase that methylate inorganic arsenic, Toxicol. Appl. Pharmacol. 140 (1996) 77–84.
[26] S.M. Healy, R.A. Zakharyan, H.V. Aposhian, Enzymatic methylation of arsenic compounds. IV. In vitro and in vivo deficiency of the methylation of arsenite and monomethylarsonic acid in the guinea pig, Mutat. Res. 386 (1997) 229–239.
[27] H.V. Aposhian, R.A. Zakharyan, M.D. Avram, A. Sampayo-Reyes, M.L. Wollenberg, A review of the enzymology of arsenic metabolism and a new potential role of hydrogen peroxide in the detoxication of the trivalent arsenic species, Toxicol. Appl. Pharmacol. 198 (2004) 327–335.
[28] G.L. Kedderis, A.R. Elmore, E.A. Crecelius, J.W. Yager, T.L. Goldsworthy, Kinetics of arsenic methylation by freshly isolated B6C3F1 mouse hepatocytes, Chem. Biol. Interact. 16 (2006) 139–145.
[29] W.W. Cleland, Steady state kinetics, in: P.D. Boyer (Ed.), The Enzymes, vol. 2, Academic Press, New York, 1970, pp. 1–65.
[30] O.A. Levander, Metabolic interrelationships between arsenic and selenium, Environ. Health Perspect. 19 (1977) 159–164.
[31] M. Styblo, D.J. Thomas, Selenium modifies the metabolism and toxicity of arsenic in primary rat hepatocytes, Toxicol. Appl. Pharmacol. 172 (2001) 52–61.
[32] R.W.J. Sarver, W.C. Krueger, An infrared and circular dichroism combined approach to the analysis of protein secondary structure, Anal. Biochem. 199 (1991) 61–67.
[33] J.T. Yang, C.S.C. Wu, H.M. Martinez, Calculation of protein conformation from circular-dichroism, Methods Enzymol. 130 (1986) 208–269.
[34] J.P. Hennessey, W.C. Johnson, Information-content in the circular-dichroism of proteins, Biochemistry 20 (1981) 1085–1094.
[35] M. Levitt, C. Chothia, Structural patterns in globular proteins, Nature 261 (1976) 552–558.
[36] S. Krimm, J. Bandekar, Vibrational spectroscopy and conformation of peptides, polypeptides, and proteins, Adv. Protein Chem. 38 (1986) 181–364.
[37] W.K. Surewicz, H.H. Mantsch, New insight into protein secondary structure from resolution-enhanced infrared-spectra, Biochim. Biophys. Acta 952 (1988) 115–130.
[38] A. Dong, P. Huang, W.S. Caughey, Redox-dependent changes in beta-extended chain and turn structures of cytochrome-*c* in water solution determined by 2nd derivative amide-I infrared-spectra, Biochemistry 31 (1992) 182–189.
[39] W.Y. Sun, J.L. Fang, M. Cheng, P.Y. Xia, W.X. Tang, Secondary structure dependent on metal ions of copper, zinc superoxide dismutase investigated by Fourier transform IR spectroscopy, Biopolymers 42 (1997) 297–303.
[40] K.J. Ghosh, S.G. Peisajovich, Y. Shai, Sendai virus internal fusion peptide: structural and functional characterization and a plausible mode of viral entry inhibition, Biochemistry 39 (2000) 11581–11592.
[41] D.M. Byler, J.N. Brouillette, H. Susi, Quantitative studies of protein structure by FTIR spectral deconvolution and curve fitting, Spectroscopy 3 (1986) 29–32.
[42] A.C. Dong, W.S. Caughey, Infrared methods for study of hemoglobin reactions and structures, Methods Enzymol. 232 (1994) 139–175.